ADVANCED MATERIALS
www.advmat.de

www.MaterialsViews.com

Silver Nanowires: From Scalable Synthesis to Recyclable Foldable Electronics

Cheng Yang, Hongwei Gu, Wei Lin, Matthew M. Yuen,* Ching Ping Wong,* Mingyong Xiong, and Bo Gao*

There is currently an urgent need for electronic devices with superior performance, robustness, smaller size, lower cost, user friendliness, and that do not increase the environmental burden.[1,2] Many materials scientists and engineers have been searching for novel flexible semiconductive materials as integrated circuits (ICs) to achieve the properties of both flexibility and stretchability.[3–8] Meanwhile, other researchers focus on the substrate materials that cater to the "chip-on-flex technologies", which are in a position of more imperative need in the current industry and consumer market.[1,9–11] Recently, Siegel et al. demonstrated the feasibility of fabricating electrical circuits on paper for the purpose of foldable and disposable devices, which displays a promising future for the low-cost consumable electronic devices.[12] Compared to the conventional printed circuit board (PCB) technology, paper offers a few advantages. For example, paper is inexpensive and can decompose easily; it is much thinner than the ordinary PCBs and can be folded, unfolded, and creased easily; electronics based on paper can be stored in smaller spaces or made to form 3D self-standing structures.[12,13] Finally, with the porous and breathable nature, paper can potentially be applied in disposable components for adhesives and clinical diagnosis, such as being combined with portable analytical devices.[14,15] However, because ordinary paper has a high average roughness (about 5 μm, which is related to the feature size of the cellulose fibers)[16] and unique mechanical and thermal properties, an appropriate technique for fabricating the paper-based electronic devices needs to be developed to replace the current patterning technique used for PCBs.[17]

Among the available printable conductive materials, Ag possesses excellent malleability, mechanical robustness, the highest electrical conductivity (1.6×10^{-6} Ω cm) among metals, and is highly resistant to corrosion. In particular, highly anisotropic silver nanowires (Ag NWs) have extra advantages in forming a percolated network when applied to rough surfaces (e.g., paper). Compared to other materials, such as nanoparticle-based conductive inks and microflake-filled conductive adhesives, which suffer from the solution leaching problem on porous paper and more easily fail under serious strains (e.g., foldings), NWs are in a better position to be used as printable conductive materials. Moreover, Ag NWs are known to be safe to human beings compared to other non-metallic conductive materials (e.g., carbon nanotubes).[18]

In order to obtain Ag NWs with high quality and productivity, considerable scientific research on their synthesis has been conducted. Xia and co-workers successfully synthesized high-quality Ag nanocubes and nanowires, in a way that ethylene glycol (EG) solutions of $AgNO_3$ and poly(vinylpyrrolidone) (PVP) are dropwisely added at 148 °C under moisture-free conditions.[19–23] When using this method, low reagent concentration and slow addition rate are necessary for controlling the quality of the 1D crystals (i.e., Ag NWs); otherwise, seed crystals with specific structures or metal salt seasoning agents are necessary.[20] The steady-state growth method is applicable to both 1D and 0D Ag crystals, such as Ag NWs and nanocubes.[21,24] Additionally, Xia and co-workers elucidated the oxidative etching mechanism of the single-crystalline Ag nanocrystals with various shapes in the presence of Cl^- and O_2 in the solvent, which shed light on some recent progress in Ag NW preparations under more convenient conditions.[19,25–27]

Here we report a facile preparation method for Ag NWs that can be conveniently scale-up. Glycerol is used as the solvent and it is seasoned with a small dose of water so as to modulate the reaction process. As glycerol has two primary hydroxyl groups and one secondary hydroxyl group, it shows stronger reducing ability compared to ethylene glycol. Moreover, its high boiling point (290 °C) renders the reduction reaction at higher temperatures feasible, which accelerates the reduction of Ag cation. Water as an electrolyte actively takes part in the charge transfer process through chemisorption and desorption,

Dr. C. Yang, Prof. M. M. Yuen, B. Gao
Department of Mechanical Engineering
The Hong Kong University of Science and Technology
Clear Water Bay, Kowloon, Hong Kong, China
E-mail: yangch@ust.hk; meymf@ust.hk
Prof. H. Gu
Key Laboratory of Organic Synthesis of Jiangsu Province
College of Chemistry
Chemical Engineering and Materials Science
Soochow University
Suzhou 215123, China
W. Lin, Prof. C. P. Wong
School of Materials Science and Engineering
Georgia Institute of Technology
771 Ferst Drive, Atlanta, GA 30332, USA
E-mail: cp.wong@mse.gatech.edu
Prof. C. P. Wong
Faculty of Engineering
The Chinese University of Hong Kong
Shatin, Hong Kong
Dr. M. Xiong
Department of Chemical and Biomolecular Engineering
The Hong Kong University of Science and Technology
Clear Water Bay, Kowloon, Hong Kong, China

DOI: 10.1002/adma.201100530

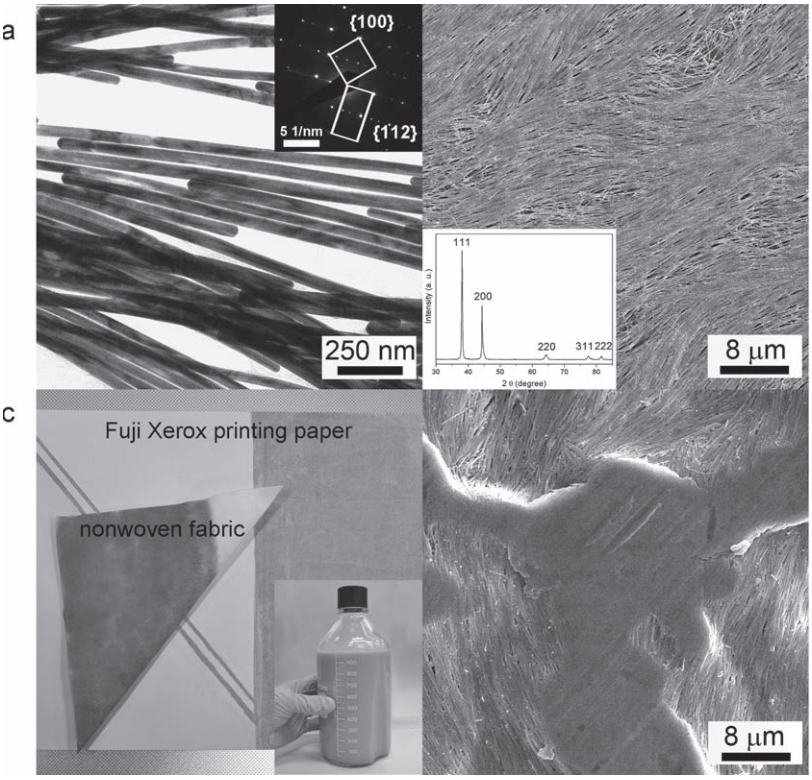

Figure 1. a) TEM images of the Ag NWs and the electron diffraction pattern of a single NW (inset). b) SEM image of the Ag NW film on a PET film. Inset: powder X-ray diffraction (XRD) spectrum of the Ag NW film. c) A photographic image of a piece of Fuji Xerox printing paper with some of the patterns of the Ag NWs (bottom). The triangle is a piece of folded nonwoven fabric that has been soaked with the Ag NWs (top). Inset: a bottle of 1 L Ag NW aqueous solution containing ≈10 g Ag NWs. d) SEM image of the Ag NW film on a piece of Fuji Xerox printing paper after hot lamination at 125 °C.

which facilitates the growth of the NWs along the {110} direction.[28,29] **Figure 1**a shows a transmission electron microscopy (TEM) image of the Ag NWs produced using this method. The NWs have uniform width and similar length (≈60 ± 20 nm in width and ≈15 ± 7 μm in length; doubly confirmed using atomic force microscopy (AFM) analysis of a large area). The selected electron diffraction pattern (Figure 1a inset) suggests that the Ag NWs are highly crystalline. A scanning electron microscopy (SEM) overview image (Figure 1b) suggests a uniform size of the Ag NWs. Figure 1c shows the photographic image of a piece of Fuji Xerox paper and a piece of nonwoven fabric (Texwipe) containing certain amount of Ag NWs that were dispensed using the Meyer rod method.[35]

Figure 2a shows the electrical resistivity of these Ag NW films with different thickness, which were drop-casted onto two kinds of paper substrates and a polyethylene terephthalate (PET) substrate. The thickness of the Ag NW film was determined by AFM (Supporting Information, Figure S4), which was averaged based on six different regions of the sample. Comparing the three results, we observe that on the rougher substrate surface, there was a higher electrical resistivity, which suggests that the rough surface disturbs the continuity of the associated Ag NW network. By adjusting the film thickness via controlling the solution concentration, we achieved 2.6×10^{-5} Ω cm of the Ag NW film (film thickness ≈2 μm), which meets the requirements for many printed conductive adhesives and inks for micro-interconnect and printed resistor applications.[30] When decreasing the film thickness on the Fuji Xerox printing paper and Fisherbrand weighing paper to less than 500 nm, we observed a higher chance of discontinuity of the film in SEM observations, which leads to higher electrical resistance correspondingly.

Paper is primarily composed of cellulose fibers, which have a fibrous structure and a diameter of a few micrometers.[31] Cellulose is the most abundant organic material in the world that is composed of the linear polysaccharide chains. Pure cellulose fibers have a high Young's modulus in the range near to 130 GPa; composites, such as papers and textiles composed of the cellulose fibers, display excellent mechanical strength and are resistant to repeated foldings. It is suggested that single crystalline Ag NW prepared using the polyol method display a higher mechanical strength (Young's modulus ≈100 GPa) than the bulk polycrystalline metal (≈83 GPa).[32,33] Considering that the Young's modulus of the Ag NW is similar to that of cellulose and the strong hydrogen bonding between each component, the film of the Ag NWs has excellently compliance to the cellulose-based paper substrate. We tentatively examined the change in electrical conductance of the circuit layer versus folding conditions on different substrates including paper and a smooth PET film. In this experiment, all samples had the thickness ≈1 μm for the

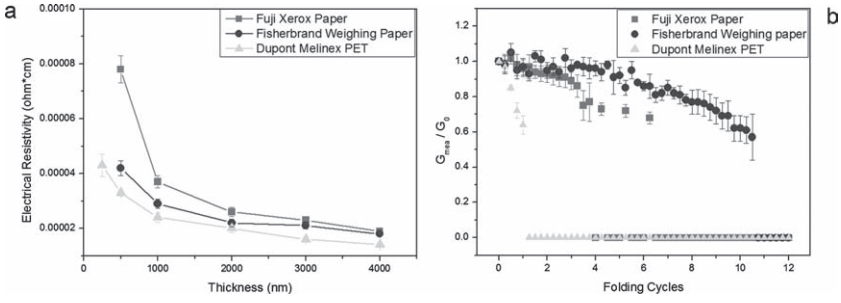

Figure 2. a) Electrical resistivity versus thickness of the Ag NW films coating on paper (Fuji Xerox and Fisherbrand) and PET (Dupont Melinex). b) Folding evaluations of the Ag-NW-based circuits on three different substrates (Fuji Xerox printing paper, Fisherbrand weighing paper, and Dupont Melinex PET film). Each consecutive data point denotes 0°, 180°, 0°, –180° (as one cycle). This figure shows 12 full cycles. The ratio of the measured conductivity (G_{mea}) to initial conductivity (G_0) of a straight line of a Ag-NW- based circuit (thickness = 1 μm, width = 2 mm) versus folding cycle (fatigue).

NW films; the electrical resistivity of the PET-based one was about 60% of the Fuji Xerox-paper-based one (as shown in Figure 2a). Then the samples were folded to ±180° and released back to 0° and then the process was repeated by loading a weight on top to achieve the folding effect. An ohm meter was used to measure the conductance of the circuit. The electrical conductance of the Ag NW films decreased with repeated folding of the paper. In Figure 2b, we observe that on the Fuji Xerox paper, there was no significant decrease in conductance when the circuit film was folded in the first three cycles, even though there were some minor fractures in the folded areas (Supporting Information, Figure S4). However, on the Fisherbrand weighing paper, the Ag NW film circuit could resist repeated foldings up to ten cycles with the decrease in G_{mea}/G_0 of about 40%. From the optical microscopy observations, there was only minor delaminating of the Ag NW film. However, the Ag NW films on the PET substrate were much fragile to resist foldings as compared to those on paper substrates, i.e., they failed after only one cycle (Figure 2b), which is related to the yield of the polymer film under strain and the weak support from the smooth PET surface. Since the smooth surface of PET film has much lower surface energy and there is no absorption effect to the Ag NWs, the latter can be easily smeared. Contrarily, the paper substrates show a strong support for the Ag NW films and the Ag NW films exhibit excellent continuity after a few folding cycles. Therefore, in real applications, additional encapsulation steps may be necessary on the PET substrates to achieve better performance. The most prominent cracks in the films followed the ruptures and displacements of the cellulose fibers, which were located in the areas with the maximum tensile strain. Repeated folding eventually produced ruptures of the Ag NW films, which correlated to the trace of crack of the paper substrate.

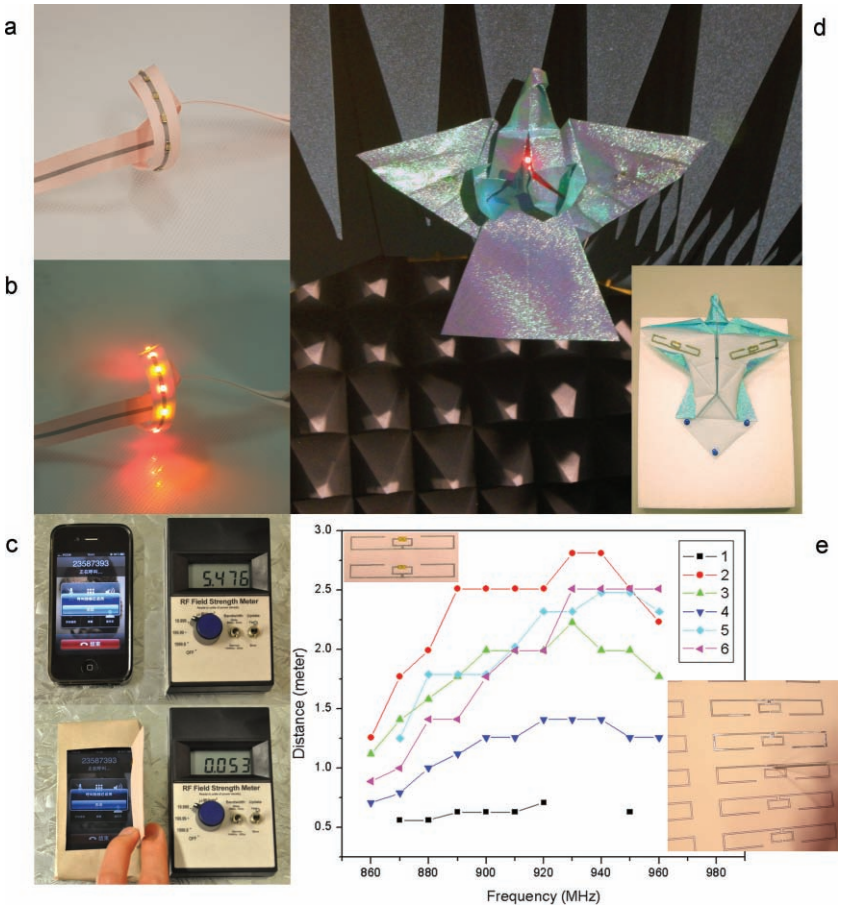

Figure 3. a,b) Photographic images showing that the Ag-NW-based circuit can support the LED chips on a piece of Fuji Xerox paper. a) No power. b) Powered by a direct current (DC). c) Photographic comparison of the radio frequency (RF) field strength when dialing an Apple iPhone 4 smartphone. Top: normal (no shielding); bottom: the cell phone is shielded with a piece of single-sided, Ag-NW-covered Fuji Xerox paper and grounded by the zinc plate substrate. d) A photographic image showing the paper angel, which contains both the RFID tags on the back (shown in the inset) and the LEDs driven by the button battery on a Ag-NW-based circuit in her chest. It is placed in an anechoic room, which is ready for RF signal read range evaluations. e) Photographic images showing the tailor-made RFID tags containing Ag-NW-based antenna and the preparation proess. Inset: the yellow parts in the center of the antenna are the straps. e) Read range analysis of the RFID tags based on the Ag NW antennas, as also reported in Table 1. Insets: preparation of and prepared RFID tags; the length of the antenna was 8.5 cm and the width was 1 mm.

The NW-paper electronics can potentially be applied to a variety of functional circuits with complex shapes and even 3D structures. For instance, we fabricated the LED chips onto a Ag NW circuit on a piece of Fuji Xerox paper (**Figure 3**a,b) using a surface-mounting technique. This luminescent strip can be repeatedly folded and twisted, so as to cater for various applications. On the other hand, we reshaped a piece of paper with a thin layer of Ag NWs into a box that holds an Apple iPhone 4 smartphone. When dialing a number, the box can effectively shield the RF signals (Figure 3c) from the smartphone. A more complicated motif, shown in Figure 3d, displays a light-weight, battery-powered "paper angel" with the LED "candles" on her chest (driven by a 3.0 V button battery) and a pair of radio frequency identification (RFID) antenna structure on the back of her wings (Figure 3d inset). We further evaluated the signal transmittance performance of the two RFID tags and some others in an anechoic room (Figure 3d); they were prepared using a film of the Ag NWs as the antenna. Figure 3e insets show the geometry of the antenna samples and the preparation process of the antennas. **Table 1** summarizes the read range performances and the corresponding electrical resistivity of some of the RFID tags with the same geometry as the antenna and the same type of chips. It appeared that the read range was inhibited when the electrical resistance of the whole length of the antenna is too high. However, when the electrical resistance was lower than about 63 Ω, the read range could reach 2 m or more. In order to further confirm the long-term reliability of the Ag-NW-based circuits for real applications, we tested the NW-based circuit samples in a humidity chamber with 85 °C/85% relative

Table 1. The electrical resistance of the whole length of the antenna and the read range distance (at 940 MHz) of some of the Ag-NW-based RFID tags. Samples are the same as in Figure 3e.

Sample	Resistance [Ω]	Distance at 940 MHz [m]
1	248.0	–
2	63.0	2.81
3	71.0	1.99
4	82.9	1.41
5 (angel wing in Figure 3)	21.2	2.48
6 (angel wing in Figure 3)	18.7	2.51

humidity conditions for 720 h. In **Figure 4**a, we observe that in the first 48 h, there is a drop in electrical resistance, which may be related to the agglomerations of the PVP residue that is attached on the Ag NW surface.[34] Later, the electrical resistance starts to increase. In a 30-day aging test, there was no significant change in the electrical resistance of the Ag NW circuit samples on different substrates. By measuring the resistance of every 40-mm distance on a piece of straight circuit (total length of 200 mm) prepared under the same conditions on the Fuji Xerox paper, we noted that they all exhibited relatively similar electrical resistance in the same length (error <10%), which suggests good homogeneity and reproducibility of the drop-casting method.

To further reduce the contact resistance among the NW network, we evaluated the possibility of hot laminating the Ag-NW-based paper circuits (at 125 °C) rather than sintering them. As shown in Figure 4b, Ag NW circuits with a controlled width (1 mm) and length (60 mm) and different thicknesses (0.5 μm, 1 μm, and 2 μm) on different substrates were laminated for three cycles, performed with a film laminator (SF-320) (Wenzhou Hongda Electrical Equip Co., Ltd) with the pressure at ≈500 kPa and the speed 100 cm min^{-1}. Sequential hot laminations resulted in a decrease in electrical resistance of approximately 10–20% of the samples. Moreover, we observe that this process is particularly effective for thicker Ag NW films, which may be related to the more evenly distributed Ag NWs in the circuits. The smoother the substrate surface, the more effective in the reduction of electrical resistance by the hot-laminations, which confirms the observation in Figure 1d that the Ag NWs are compatible with the roughness of the paper substrate. Additionally, we studied the feasibility of enzymatic recycling of the paper-based RFID tag (with the Ag-NW-based antennas; Supporting Information Figure S3). It appeared that the Ag NWs from the precipitate residues maintained their electrical conductivity, while the organic parts decomposed into small molecules such as ethanol.

In summary, we have developed a facile synthetic technique for large-scale production of high-quality Ag NWs that is simple, environmentally benign, and has a wide processing window for achieving high yield. This technique ensures an extensive application of NWs as electrical circuits and interconnects in flexible consumable electronics, together with better performance and lower cost. Conductive films formed by the Ag NWs exhibit electrical conductivity (≈5×10^6 S m^{-1}), which is close to that of eutectic solders, renders them a competitive alternative as the electric current carrier. They are able to form uniform conductive circuits on various low-cost and rough substrates to support available electronic components, which is an advantage in the blooming flexible electronics technology. The Ag-NW-based circuits may display many unique characters, including low-temperature processability, foldability, high reliability, lightweight, low cost, mechanical robustness, recyclability, and 3D reconfigurability. When further furnishing the available materials with appropriate printing and packaging techniques, we envision them to have versatile consumer electronic applications.

Experimental Section

Ag NWs were prepared in a modified polyol reduction process. Briefly, a small dose of water was added to modulate the ripening of the seeding process. PVP was added to the glycerol solution and sodium chloride (NaCl) was used to assist the oxidative etching process. The reaction flask was then immersed into a heating mantle equipped with a polytetrafluoroethylene (PTFE) paddle stirrer. The solution temperature was raised from room temperature to 210 °C in 20 min. The color of the solution turned from pale white into light brown, red, dark gray, and eventually gray-green (near ≈200 °C). When the temperature reached 210 °C, the heating was stopped and the temperature returned to room temperature. Water was added to the solution and the mixture was centrifuged at 8000 rpm. The as-obtained Ag NWs were washed with water three times to remove the PVP residue. The Ag NWs obtained in this way have a length of ≈15 μm and a diameter of ≈60 nm (yield >95% by molar); rarely, Ag nanoparticles were observed. Ag NWs were collected and dispersed into an aqueous solution of 10 mg mL^{-1}. A broad processing window also resulted in a similar high yield; negligible yield differences were observed when scaling the reaction batch to several liters. A JEOL 6300 SEM at 15 kV was used to study the Ag NWs and their films on paper. TEM (JEOL 2010) at 200 kV was used to analyze the Ag NWs. The cross sections were prepared using a Leica ultracut-R ultra-microtome. Powder XRD spectra of the Ag NW films were obtained using a PAnalytical X-ray Diffractometer, Model X'pert Pro. The film thickness was determined using AFM on a Nanoscope-MultiMode/Dimension (Digital Instruments). A detailed description of the synthesis route and analysis is included in the Supporting Information.

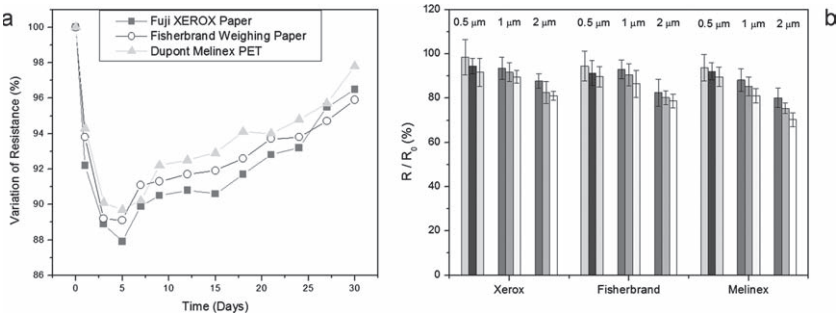

Figure 4. a) Variation of the electrical resistance over time under 85 °C/85 relative humidity conditions for 720 h. Film thickness = 2 μm. b) Variation in the electrical resistance after the hot lamination process on different substrate materials. The thickness of the Ag NW film is listed above each column. The consecutive columns from left to right are of 1, 2, and 3 cycles of lamination.

Supporting Information

Supporting Information is available from the Wiley Online Library or from the author.

Acknowledgements

The authors thank the financial support from RGC No. 621810 (Hong Kong government).

Received: February 9, 2011
Revised: March 28, 2011
Published online: May 17, 2011

[1] R. Das, P. Harrop, Printed, Organic & Flexible Electronics Forecasts, Players & Opportunities 2009–2029, IDTechEx, Cambridge, MA **2009**.
[2] S. R. Forrest, *Nature* **2004**, *428*, 911.
[3] X. M. Lu, Y. N. Xia, *Nat. Nanotechnol.* **2006**, *1*, 163.
[4] K. Takei, T. Takahashi, J. C. Ho, H. Ko, A. G. Gillies, P. W. Leu, R. S. Fearing, A. Javey, *Nat. Mater.* *9*, 821.
[5] Y. G. Sun, W. M. Choi, H. Q. Jiang, Y. G. Y. Huang, J. A. Rogers, *Nat. Nanotechnol.* **2006**, *1*, 201.
[6] Z. Y. Fan, H. Razavi, J. W. Do, A. Moriwaki, O. Ergen, Y. L. Chueh, P. W. Leu, J. C. Ho, T. Takahashi, L. A. Reichertz, S. Neale, K. Yu, M. Wu, J. W. Ager, A. Javey, *Nat. Mater.* **2009**, *8*, 648.
[7] S. I. Park, Y. J. Xiong, R. H. Kim, P. Elvikis, M. Meitl, D. H. Kim, J. Wu, J. Yoon, C. J. Yu, Z. J. Liu, Y. G. Huang, K. Hwang, P. Ferreira, X. L. Li, K. Choquette, J. A. Rogers, *Science* **2009**, *325*, 977.
[8] K. Takei, T. Takahashi, J. C. Ho, H. Ko, A. G. Gillies, P. W. Leu, R. S. Fearing, A. Javey, *Nat. Mater.* **2010**, *9*, 821.
[9] F. Barlow, A. Lostetter, A. Elshabini, *Microelectron. Reliab.* **2002**, *42*, 1091.
[10] S. P. Lacour, J. Jones, S. Wagner, T. Li, Z. G. Suo, *Proc. IEEE* **2005**, *93*, 1459.
[11] D. H. Kim, Y. S. Kim, J. Wu, Z. Liu, J. Song, H. S. Kim, Y. Y. Huang, K. C. Hwang, J. A. Rogers, *Adv. Mater.* **2009**, *21*, 3703.
[12] A. C. Siegel, S. T. Phillips, M. D. Dickey, N. S. Lu, Z. G. Suo, G. M. Whitesides, *Adv. Funct. Mater.* **2010**, *20*, 28.
[13] C. A. Harper, *Electronic Packaging and Interconnection Handbook*, McGraw-Hill, New York **2005**.
[14] A. W. Martinez, S. T. Phillips, M. J. Butte, G. M. Whitesides, *Angew. Chem. Int. Ed.* **2007**, *46*, 1318.
[15] A. W. Martinez, S. T. Phillips, G. M. Whitesides, *Proc. Natl. Acad. Sci. USA* **2008**, *105*, 19606.
[16] R. A. Young, R. M. Rowell, *Cellulose: structure, modification, and hydrolysis*, Wiley, New York **1986**.
[17] R. S. Khandpur, *Printed circuit boards: design, fabrication, assembly and testing*, McGraw-Hill, New York **2006**.
[18] Y. H. Bai, Y. Zhang, J. P. Zhang, Q. X. Mu, W. D. Zhang, E. R. Butch, S. E. Snyder, B. Yan, *Nat. Nanotechnol.* **2010**, *5*, 683.
[19] B. Wiley, Y. Sun, Y. Xia, *Acc. Chem. Res.* **2007**, *40*, 1067.
[20] B. Wiley, Y. G. Sun, B. Mayers, Y. N. Xia, *Chem. Eur. J.* **2005**, *11*, 454.
[21] Y. G. Sun, B. Mayers, T. Herricks, Y. N. Xia, *Nano Lett.* **2003**, *3*, 955.
[22] Y. N. Xia, P. D. Yang, Y. G. Sun, Y. Y. Wu, B. Mayers, B. Gates, Y. D. Yin, F. Kim, Y. Q. Yan, *Adv. Mater.* **2003**, *15*, 353.
[23] K. E. Korte, S. E. Skrabalak, Y. Xia, *J. Mater. Chem.* **2008**, *18*, 437.
[24] B. Wiley, T. Herricks, Y. G. Sun, Y. N. Xia, *Nano Lett.* **2004**, *4*, 1733.
[25] Y. Xia, Y. J. Xiong, B. Lim, S. E. Skrabalak, *Angew. Chem. Int. Ed.* **2009**, *48*, 60.
[26] X. L. Tang, M. Tsuji, P. Jiang, M. Nishio, S. M. Jang, S. H. Yoon, *Colloids Surf., A* **2009**, *338*, 33.
[27] L. F. Gou, M. Chipara, J. M. Zaleski, *Chem. Mater.* **2007**, *19*, 1755.
[28] A. Montoya, B. S. Haynes, *J. Phys. Chem. C* **2007**, *111*, 1333.
[29] C. Qin, J. L. Whitten, *J. Phys. Chem. B* **2005**, *109*, 8852.
[30] S. De, T. M. Higgins, P. E. Lyons, E. M. Doherty, P. N. Nirmalraj, W. J. Blau, J. J. Boland, J. N. Coleman, *ACS Nano* **2009**, *3*, 1767.
[31] J. C. Roberts, *The Chemistry of Paper*, Royal Society of Chemistry, Cambridge **1996**.
[32] A. Heidelberg, L. T. Ngo, B. Wu, M. A. Phillips, S. Sharma, T. I. Kamins, J. E. Sader, J. J. Boland, *Nano Lett.* **2006**, *6*, 468.
[33] P. Zadorecki, H. Karnerfors, *Compos. Sci. Technol.* **1986**, *27*, 291.
[34] J. L. Elechiguerra, L. Larios-Lopez, C. Liu, D. Garcia-Gutierrez, A. Camacho-Bragado, M. J. Yacaman, *Chem. Mater.* **2005**, *17*, 6042.
[35] L. B. Hu, H. S. Kim, J. Y. Lee, P. Peumans, Y. Cui, *ACS Nano* **2010**, *4*, 2955.